JBC Papers in Press. Published on February 25, 2011 as Manuscript M111.233916
The latest version is at http://www.jbc.org/cgi/doi/10.1074/jbc.M111.233916

THE HUMAN HYALURONAN SYNTHASE 2 GENE AND ITS NATURAL ANTISENSE RNA EXHIBIT COORDINATED EXPRESSION IN THE RENAL PROXIMAL TUBULAR EPITHELIAL CELL*

Daryn R Michael[1], Aled O Phillips[1,2], Aleksandra Krupa[1], John Martin[1,2], James E Redman[3], Abdalsamed Altaher[1], Rachel D Neville[1,2], Jason Webber[1], Min-young Kim[1,], and Timothy Bowen[1,2***]**

From the [1]Institute of Nephrology, Cardiff University School of Medicine, Heath Park, Cardiff CF14 4XN, UK
[2]Cardiff Institute of Tissue Engineering and Repair, Cardiff Medicentre, Heath Park, Cardiff CF14 4UJ, UK
[3]School of Chemistry, Cardiff University, Park Place, Cardiff CF10 3AT, UK

Running head: Coordinated expression of HAS2 and HAS2-AS1

***Address correspondence to: Timothy Bowen, Institute of Nephrology,
Cardiff University School of Medicine, Heath Park, Cardiff CF14 4XN, UK
Tel.: 44-29-2074-8389; Fax: 44-29-2074-8470; E-mail: bowent@cf.ac.uk

Aberrant expression of the human hyaluronan synthase 2 (*HAS2*) gene has been implicated in the pathology of malignancy, pulmonary arterial hypertension, osteoarthritis, asthma, thyroid dysfunction and large-organ fibrosis. Renal fibrosis is associated with increased cortical synthesis of hyaluronan (HA), an extracellular matrix glycosaminoglycan, and we have shown that HA is a correlate of interstitial fibrosis *in vivo*. Our previous *in vitro* data have suggested that both HAS2 transcriptional induction and subsequent HAS2-driven HA synthesis may contribute to kidney fibrosis via phenotypic modulation of the renal proximal tubular epithelial cell (PTC). Post-transcriptional regulation of HAS2 mRNA synthesis by natural antisense RNA HAS2-AS1 has recently been described in osteosarcoma cells, but the antisense transcript was not detected in kidney. In the present study, PTC stimulation with interleukin-1β (IL-1β) or transforming growth factor-β1 (TGF-β1) induced coordinated temporal profiles of HAS2-AS1 and HAS2 transcription. Constitutive activity of the putative HAS2-AS1 promoter was demonstrated, and transcription factor binding sequence motifs were identified. Knockdown of Sp1/Sp3 expression by siRNA blunted IL-1β-induction of both HAS2-AS1 and HAS2, and Smad2/Smad3 knockdown similarly attenuated TGF-β1 stimulation. Inhibition of IL-1β-stimulated HAS2-AS1 RNA induction using HAS2-AS1-specific siRNAs also suppressed up-regulation of HAS2 mRNA transcription. The thermodynamic feasibility of HAS2-AS1:HAS2 heterodimer formation was demonstrated *in silico*, and locus-specific cytoplasmic double-stranded RNA was detected *in vitro*. In summary, our data show that transcriptional induction of HAS2-AS1 and HAS2 occurs simultaneously in PTC, and suggest that transcription of the antisense RNA stabilises or augments HAS2 mRNA expression in these cells via RNA:mRNA heteroduplex formation.

The linear, non-sulphated glycosaminoglycan hyaluronan (HA) is a ubiquitous component of the vertebrate extracellular matrix (ECM) with a multiplicity of cellular functions in both physiological and pathophysiological contexts (1-8). HA is synthesised at the cell membrane by the HA synthase (HAS) enzymes, encoded in humans by the corresponding multi-gene family *HAS1-3* (9-11).

Frequently associated with the fibrotic response in major organs, HA is a highly effective biomarker for liver fibrosis (12,13). Similarly, in lung fibrosis, accumulation of HA has been observed (14,15), and in some cases up-regulated HAS2 transcription has also been reported (14). For all progressive renal diseases, the rate of progression correlates with the degree of corticointerstitial fibrosis. Increased HA synthesis and ECM expansion in the renal corticointerstitium is a common feature of kidney fibrosis (16), and our recent studies on renal biopsy samples from diabetic nephropathy patients demonstrate that HA is a correlate of interstitial fibrosis *in vivo* (17). A number of our *in vitro* studies have suggested that HA may contribute to renal fibrosis via the regulation of renal proximal tubular epithelial cell (PTC) phenotype and differentiation of fibroblast to myofibroblast (18,19), processes in which up-regulated HAS2 transcription may also play a role (20,21).

The *HAS2* gene, with the current reference mRNA sequence NM_005328.2, is located at 8q24.13 on the minus strand of human chromosome 8 and spans positions 122,625,271 to 122,653,630 according to the February 2009 freeze at the UCSC Genome Bioinformatics site (http://genome.ucsc.edu/). Our work has extended this HAS2 reference mRNA sequence by 130 upstream nucleotides (22), and shown that the ubiquitously expressed zinc finger transcription factors specificity protein (Sp) Sp1 and Sp3 bind to multiple recognition sites upstream of this repositioned transcription start site to mediate constitutive HAS2 transcription (23). In collaboration, we have also described activity at the HAS2 promoter of retinoic acid response elements (RAREs) in response to *all-trans* retinoic acid (ATRA), and of nuclear factor (NF)-κB following tumour necrosis factor-α stimulation (24); ATRA- and forskolin-stimulated complexes of RAREs and cAMP response element binding protein (CREB)-1 have also been reported (25).

Post-transcriptional regulation of HAS2 expression by a tetraexonic RNA, transcribed from the opposite genomic DNA strand at the *HAS2* locus, has been described by Chao and Spicer (26). This transcript was originally called HASNT, for **HA s**ynthase 2 a**nt**isense (26), but has since been annotated formally with the NCBI Entrez Gene definition HAS2-AS1 HAS2 antisense RNA (non-protein coding) [*Homo sapiens*]. The most recent HAS2-AS1 reference sequence has the NCBI accession number NR_002835.2, and is located on the plus strand of human chromosome 8 from positions 122,651,586 to 122,657,564. HAS2-AS1 exon 2 shares sequence complementarity with the first exon of the *HAS2* gene (see Fig. 1*A*, below). Over-expression of this complementary antisense region has been shown to down-regulate HAS2 transcription and HA synthesis in osteosarcoma cells, but the antisense transcript was not detected in kidney (26).

The aim of the present study was to identify the expression of HAS2-AS1 in PTC and then to investigate the role of this RNA in the post-transcriptional regulation of HAS2 expression in these cells. Having established that HAS2-AS1 was transcribed in PTC, subsequent time-course analyses showed coordinated up-regulation of HAS2 and HAS2-AS1 transcription in response to stimulation with the pro-inflammatory cytokine interleukin (IL)-1β or the key fibrotic regulator transforming growth factor (TGF)-β1. We then set out to identify the factors regulating this simultaneous sense and antisense expression, and to analyse the effects on HAS2 expression of modulating HAS2-AS1 transcription in these cells. Finally, we investigated the thermodynamic feasibility of HAS2-AS1:HAS2 heterodimer formation *in silico* and detected locus-specific ribonuclease-resistant double-stranded RNA, providing evidence for the formation of RNA:mRNA duplexes *in vitro*.

EXPERIMENTAL PROCEDURES

Figure 1

Cell Culture—Culture of human PTC line HK-2 was as described previously (22). Recombinant IL-1β and TGF-β1 were obtained from R&D Systems Europe Ltd. (Abingdon, Oxfordshire, UK) and were used in accordance with guidance from the manufacturer.

Reverse Transcription (RT) and Endpoint RT-PCR—Extraction of total (22) as well as nuclear and cytoplasmic (27) RNAs was carried out as described previously. Nuclear and cytoplasmic RNA extracts were treated with 20 U/ml of DNase (Promega UK Ltd, Southampton, Hampshire, UK) and, where appropriate, 100 μg/ml of RNase A (Roche Diagnostics Ltd, Burgess Hill, West Sussex, UK) at 37°C for 2 h. First strand cDNA synthesis from 0.5 - 1 μg of total RNA was performed using the cDNA Reverse Transcriptase High Capacity Kit from Applied Biosystems (Warrington, Cheshire, UK). Endpoint RT-PCR primers were designed to span intron-exon boundaries to obviate amplification from contaminating genomic DNA, with the exception of the oligonucleotides used in heteroduplex detection, sequence data for which are given in the legend to Fig. 8*B*. Details of all other HAS2-AS1-specific primer sequences / binding sites are shown in Fig. 1*B*. All oligonucleotides were obtained from Invitrogen Ltd. (Paisley, Renfrewshire, UK) or Metabion (Martinsried, Bavaria, Germany). As we have detailed elsewhere, endpoint RT-PCR reactions were carried out, their

products visualised and, where appropriate, gel fragments were purified and sequenced to confirm the identity of both HAS2-AS1-related products and products of non-specific amplification (22).

RT and SYBR Green Quantitative RT-PCR (qRT-PCR) Analysis of HAS2-AS1—Our SYBR Green qRT-PCR assay for HAS2-AS1 was optimised for linear detection with an efficiency of approximately 100% using the oligonucleotide primers shown in Fig. 1*B*. Total RNA was isolated as outlined above, and followed by a HAS2-AS1-specific RT step using 250 ng - 2 μg of total RNA and the SYBR-RT primer at a final concentration of 100 nM, 500 nM, or 1.0 μM. RT was carried out at 45˚C for 5 min, 37˚C for 1 h and 85˚C for 5 min, followed by chilling at 4˚C. qRT-PCR was then performed in a total reaction volume of 20 μl using 1.3 μl of cDNA, the Power SYBR Green PCR Master Mix (Applied Biosystems) and HAS2-AS1-specific PCR primers SYBR-F and SYBR-R at a final concentration of 300 nM. Samples were processed in Applied Biosystems Fast Optical 96-well reaction plates in a 7900HT Fast Real-Time PCR System (Applied Biosystems) with cycling parameters of 95˚C for 10 min followed by 40 cycles of 95˚C for 15 s and 60˚C for 1 min. Melting curve analysis was performed to confirm amplification of a single product. Following optimisation, routine HAS2-AS1 analyses were carried out using reverse transcription from 1 μg of total RNA, followed by qRT-PCR as described above. Onboard SDS v2.3 software was used for the analysis of output data from biological triplicates.

qRT-PCR using Taqman Assays—Taqman assays for HAS2 (catalogue number Hs00193435_m1), Smad2 (HS00183425_M1), Smad3 (HS00232222_M1), Sp1 (Hs00412720_m1), Sp3 (Hs01595811_m1) and 18S rRNA (4310893E) were obtained from Applied Biosystems. A custom HAS2-AS1 TaqMan assay (HAS2-AS1_LS) was also purchased from Applied Biosystems and used, as recommended by the manufacturer, to analyse cDNA generated from subsequent siRNA knockdown experiments. For HAS2 and 18S rRNA qRT-PCR, 1 μl of cDNA was added to 19 μl of a qRT-PCR reaction mix in 1 x Taqman Fast Universal PCR Master Mix (Applied Biosystems), 2 μl of cDNA was added to 18 μl for the corresponding HAS2-AS1 reaction. Biological triplicates of all Taqman assays were analysed as outlined above.

Absolute quantification of HAS2 and HAS2-AS1 copy numbers using SYBR Green qRT-PCR—Absolute quantification of HAS2 mRNA was carried out by standard means using the HAS2 open-reading frame (a gift from Dr AP Spicer, Texas A&M University System Health Center, Houston, TX, USA) inserted into an expression vector that we have described elsewhere (28), and oligonucleotide sequences aqHAS2-F: tagaagaagatcccatggttgg and aqHAS2-R: ggaatgagatccaggaatcgta. HAS2-AS1 RNA was quantified similarly using the full length antisense sequence in pBluescript (Epoch Biolabs Inc., Missouri City, TX, USA) together with oligonucleotide primer sequence aqHAS2-AS1F and an oligonucleotide binding at the site aqHAS2-AS1R shown in Fig. 1*B*.

HAS2-AS1 Luciferase Reporter Analysis—Putative HAS2-AS1 promoter sequences were PCR-amplified using primers / primer binding-sites highlighted in Fig. 1*B*, high-fidelity Platinum *Pfx* DNA polymerase (Invitrogen Ltd.) and the cycling parameters recommended by the manufacturer. Sense-strand primers 0.1-0.7 (KpnI) and the antisense-strand primer R (NotI) bore tails suitable for restriction endonuclease digestion and subsequent ligation into a modified pGL-3 luciferase reporter vector after which they were sequenced to ensure fidelity of amplification, as described previously (29). Transient transfection into HK-2 cells cultured in 6-well plates (BD Biosciences, Oxford, Oxfordshire, UK) was carried out using Lipofectamine LTX and Plus Reagent (Invitrogen Ltd.) in accordance with the manufacturer's advice. The ability of each HAS2-AS1 promoter fragment to drive transcription of the firefly luciferase gene was tested, according to the manufacturer's instructions, using the Dual-Luciferase Reporter Assay System (Promega UK Ltd., Southampton, Hampshire, UK). In each test sample, in addition to the above firefly luciferase activity, this assay also detected the *Renilla reniformis* luciferase activity of a second vector that was co-transfected to control for variation in

transfection efficiency. The relative luciferase activity of the test constructs was then expressed as the ratio of firefly : *Renilla* luciferase activities. We have described the growth medium to maximize luciferase output elsewhere (22).

siRNA Knockdown of Gene Expression—Annealed oligonucleotide siRNA reagents for the knockdown of Smad2 (catalogue number 107875), Smad3 (115717), Sp1 (143158) and Sp3 (115337) and scrambled negative control transfection (4611) were purchased from Applied Biosystems and used in accordance with the manufacturer's guidelines. Three custom siRNAs specific for HAS2-AS1, and not for HAS2, were purchased from Applied Biosystems (295471, 295472, 295473). A final concentration of 30 nM of each siRNA was transfected into HK-2 cells cultured in 12-well plates (BD Biosciences) using siPORT amine transfection reagent as described previously (23). The previously determined time-points of 3 h for IL-1β and 48 h for TGF-β1 were used for subsequent cytokine stimulations.

Sequence Data Base Analysis—HAS2-AS1 locus sequences were retrieved from the genome browser at the UCSC Genome Bioinformatics Site and analyzed for the presence of putative transcription factor binding sites (TFBSs) using the CISTER program (30) and the updated MatInspector program from the Genomatix suite (31). Selected putative TFBSs are shown in Fig. 1*B*.

Secondary structure investigations—The secondary structures of HAS2 mRNA and HAS2-AS1 RNA were investigated *in silico* to verify the thermodynamic feasibility of interaction to form a heterodimer. Minimum free energy and partition function calculations were performed using the Vienna suite of programs to probe the relative stabilities of folded RNA monomers, homo- and heterodimers (32, 33).

Statistical Analysis of Promoter Activity Assay Data—Data were calculated as the ratio of the firefly luciferase activity for each HAS2-AS1 promoter reporter construct to the corresponding value for the co-transfected *Renilla reniformis* luciferase vector. Where appropriate, statistical analysis was performed using the Wilcoxon signed rank test, and $p<0.05$ was considered statistically significant.

Statistical Analysis of qRT-PCR Data—Fold changes in expression were calculated using $2^{-(\Delta Ct1 - \Delta Ct2)}$, where ΔCt represents the difference between threshold cycle (Ct) for each target gene and 18S rRNA (34). Values for p were calculated by t-test using Microsoft Excel and were considered significant below 0.05.

RESULTS

Figure 2

PCR analysis of HAS2-AS1—Fig. 2*A* shows that, following reverse-transcription from total PTC RNA, HAS2-AS1 RNA-specific amplification was detected by endpoint RT-PCR using primers spanning two intron-exon junctions. We then optimised a SYBR Green qRT-PCR assay from which the typical amplification data shown in Fig. 2*B* were obtained, and the melting curve of the products generated is shown in Fig. 2*C*. Both of these figures demonstrate that the amplification from negative control reactions, including any contaminating genomic DNA remaining in the RNA extracts, was negligible. Fig. 2*D* illustrates that, using this assay, the detection of HAS2-AS1 was quantitative within the range of 250 ng - 2 μg of total PTC input RNA for the three reverse transcription primer concentrations shown. The absolute quantification of HAS2 and HAS2-AS1 RNAs shown in Fig. 2*E* showed that the ratio of mRNA:RNA was 4.7:1 in quiescent HK-2 cells and 4.4:1 in IL-1β-stimulated cells.

Figure 3

Expression of HAS2-AS1 and HAS2 in response to cytokine stimulation—Time courses following the expression of HAS2-AS1 and HAS2 by qRT-PCR in response to stimulation of PTC with IL-1β are shown in Fig. 3*A* and Fig. 3*B*, respectively. An initial peak of HAS2-AS1 and HAS2 expression was seen around 2 - 3 h. The expression of both RNAs then declined rapidly after 6 h before rising steadily through 48 h. Fig. 3*C* and Fig. 3*D* show that the addition of TGF-β1 also lead to the up-regulation of both transcripts in a coordinated fashion, increasing over time points to 72 h.

Figure 4

Promoter activity analysis of genomic DNA sequences upstream of HAS2-AS1 NR_002835—Each luciferase reporter construct containing an insert of putative HAS2-AS1 promoter sequence showed significant luciferase activity in comparison to the promoterless pGL-3 basic control vector, as seen in Fig. 4. The magnitude of activity varied from approximately 5-fold greater than pGL-3 for the 0.1 kb vector to >10-fold greater for the 0.7 kb construct. The ability of these inserts to drive the transcription of the luciferase gene demonstrated constitutive promoter activity of each and implied the presence of the HAS2-AS1 proximal promoter.

All insert sequences spanned a putative TFBS for both Sp1 and Sp3, mediators of constitutive HAS2 transcription (23), and a binding element for Smad proteins, the transcriptional factors that mediate response to TGF-β. These motifs were identified *in silico* within the first 100 nucleotides upstream of HAS2-AS1 NR_002835 (see Fig. 1*B*).

Figure 5

Stimulated HAS2-AS1 and HAS2 expression following siRNA knockdown of transcription factors—Combined transcription factor siRNAs for either Sp1/Sp3 or Smad2/Smad3 were administered prior to the addition of IL-1β or TGF-β1, respectively. The knockdown of Sp1 and Sp3 mRNAs inhibited IL-1β-stimulated up-regulation of HAS2 (Fig. 5*A*) and HAS2-AS1 (Fig. 5*B*), this effect was also seen when Smad2 and Smad3 mRNAs were knocked down and the induction of HAS2 by TGF-β1 was blunted (Fig. 5*C* and Fig. 5*D*).

Figure 6

Stimulated HAS2-AS1 and HAS2 expression following siRNA knockdown of HAS2-AS1—Low abundance HAS2-AS1 expression was detected in quiescent PTC. Therefore, the effectiveness of HAS2-AS1 siRNA knockdown was evaluated following transcriptional induction by IL-1β, which repeatedly induced a greater magnitude of up-regulation of HAS2-AS1 transcription than TGF-β1 (see Fig. 3 and Fig. 5). Each of the three siRNAs analysed significantly inhibited IL-1β induction of HAS2-AS1 RNA, as shown in Fig. 6*A*. In addition, Fig. 6*B* shows that each siRNA also blunted the up-regulation of HAS2 mRNA synthesis, but this inhibitory effect was only statistically significant in two out of three cases.

Figure 7

Endpoint RT-PCR analysis of HAS2-AS1 splice variants—The original description of HAS2-AS1 reported alternative splicing of HAS2-AS1 exon 2 resulting in "long" (L-) and "short" (S-) HAS2-AS1 isoforms varying in length by 83 nucleotides and sharing either 257 nucleotides (L-) or 174 nucleotides (S-) of complementary sequence with the first exon of HAS2, respectively (see Fig. 7*A*) (26). Fig. 7*B* shows the detection of both L- and S-HAS2-AS1 expression in PTC by agarose gel electrophoresis of endpoint RT-PCR-amplified fragments. For L-HAS2-AS1-specific reactions A-C and B-F, oligonucleotides were designed to prime amplification from the 83 nucleotide alternatively spliced region of exon 2. S-HAS2-AS1-specific products were amplified using primers A-D and E-F.

Figure 8

Thermodynamic feasibility of HAS2-AS1:HAS2 heterodimer formation and heteroduplex detection—HAS2 mRNA and HAS2-AS1 RNA were predicted to interact primarily through duplex formation of their perfectly complementary regions (174 nucleotides for S-HAS2-AS1 and 257 nucleotides for L-HAS2-AS1), with little other intermolecular hybridization predicted between the sequences (Fig. 8*A*). Based on the ensemble free energies of the species, at equilibrium at 37ºC an equimolar mixture of HAS2 mRNA and L-HAS2-AS1 was predicted to exist overwhelmingly as a heterodimer (-2180 kcal/mol) without competition from homodimers (-2055 and -1696 kcal/mol for HAS2 mRNA and L-HAS2-AS1 respectively) or intramolecularly folded monomeric forms (-1022 and -841 kcal/mol for HAS2 mRNA and L-HAS2-AS1 respectively). Comparable results were obtained for the interaction of HAS2 mRNA with S-HAS2-AS1 (data not shown). The calculations therefore support the existence of a dimer of HAS2 mRNA and HAS2-AS1 RNA in the absence of sequestration of the RNAs in kinetic or thermodynamic traps which were not considered by this analysis. The RT-PCR assay data shown in Fig. 8*B* depict the detection of a ribonuclease- and

deoxyribonuclease-resistant HAS2-AS1:HAS2 heteroduplex in PTC cytoplasmic RNA. Very little duplex signal was detected in nuclear RNA extracts (data not shown).

DISCUSSION

Understanding the mechanisms that regulate the expression of the human *HAS* genes is part of an ongoing series of studies in our laboratory that aims to determine the pathogenic mechanisms underlying renal fibrosis. In the present investigation, we analysed the expression of the HAS2 natural antisense RNA, HAS2-AS1, and investigated its role in the regulation of HAS2 expression.

Since the prescient identification of HAS2-AS1 as a post-transcriptional regulator of HAS2 expression and HA synthesis (26), a more detailed knowledge of the transcriptional output of the human genome has been revealed, including the pan-genomic significance of noncoding RNAs on gene expression (35,36). Indeed, numerous subsequent reports have suggested that cell phenotype is a function of the total transcriptome (35-38). There is also a growing appreciation of the widespread occurrence of long noncoding RNAs, including antisense transcripts like HAS2-AS1, and that their impact on gene expression is likely to vary depending on genomic locus and cellular context (38-40). Therefore, following previous data describing the down-regulation of HAS2 and HA synthesis by HAS2-AS1 in osteosarcoma cells (26), in the present investigation we analysed the expression of this natural antisense RNA in PTC.

Endpoint RT-PCR data confirmed the presence of HAS2-AS1 expression in PTC. Subsequent absolute quantification revealed that constitutive HAS2-AS1 was expressed in low copy number, particularly in quiescent HK-2 cells, and that the HAS2:HAS2-AS1 ratio in both quiescent and IL-β-stimulated cells was approximately 4.5:1.

Our qRT-PCR assay showed that the induction of HAS2 sense and HAS2-AS1 antisense transcription occurred simultaneously in response to stimulation with IL-1β or TGF-β1. Correlated expression of overlapping sense:antisense transcripts has been reported in the expression of rat inducible nitric oxide synthase (iNOS), where iNOS mRNA is stabilised by interaction with a natural antisense iNOS RNA (41). The biphasic response to IL-1β seen in Fig. 3*A* and 3*B* has been shown previously in the PTC line HK-2 (42). Luo and colleagues demonstrated that short-term IL-1β treatment inhibited Smad2/3-mediated TGF-β signalling via rapid and transient NF-κB activation, but that longer term IL-1β exposure augmented the endogenous/exogenous TGF-β-stimulated Smad response, following a switch in NF-κB nuclear subunit composition (42).

To analyse further the mechanisms regulating co-expression of HAS2-AS1 and HAS2, we created a nested series of putative promoter luciferase reporter constructs amplified from the genomic DNA upstream of the 5' end of the NR_002835 HAS2-AS1 RNA sequence. As demonstrated previously in our identification of the HAS2 promoter (22), our data suggested that sufficient of the HAS2-AS1 proximal promoter was contained in all vectors to drive luciferase gene transcription.

Analysis *in silico* showed that all inserts spanned Sp1/Sp3 and Smad consensus motifs. The suppression of induction of both HAS2 and HAS2-AS1 by IL-1β or TGF-β1 following siRNA knockdown of Sp1/Sp3 or Smad2/Smad3, respectively, was consistent with these *in silico* data. This suggested that cytokine-stimulated up-regulation of HAS2-AS1 and HAS2 transcription involved simultaneous binding of these transcription factors at both proximal promoters at the *HAS2-AS1*/*HAS2* locus.

These data supported our previous findings that Sp1 and Sp3 mediate constitutive transcription of HAS2, which is down-regulated following siRNA knockdown of these transcription factors (23). The additional observation from the present study that IL-1β-induction of HAS2 transcription was also suppressed by the mRNA knockdown of these ubiquitous transcription factors implied that Sp1 and Sp3 might perform a gatekeeper role in the transcriptional induction of HAS2 mRNA. However, since HAS2-AS1 was expressed constitutively at low abundance, the same

conclusion could not be drawn for the antisense RNA in these cells.

The simultaneous abrogation of induction of both HAS2-AS1 and HAS2 by HAS2-AS1-specific siRNAs suggested that the antisense RNA stabilised or augmented HAS2 expression in PTC. Very similar siRNA data have been reported in neuroblastoma cells from a study on β-site amyloid precursor protein-cleaving enzyme 1 (BACE-1), a candidate gene for Alzheimer's Disease that may drive disease-associated pathology (43). Furthermore, BACE-1 mRNA expression was coordinately up-regulated *in vitro* by increased transcription of the natural antisense RNA BACE-1-AS in response to cell stressors (43).

In contrast to the above, Chao and Spicer (26) showed that over-expression of HAS2-AS1 in osteosarcoma cells down-regulated both HAS2 mRNA synthesis and subsequent HA synthesis, underlining the importance of cellular context in sense:antisense interactions (38-40).

We identified in PTC both known HAS2-AS1 splice variants (26). L-HAS2-AS1 shares 257 nucleotides of complementary sequence with HAS2 exon 1, the corresponding region for S-HAS2-AS1 is 183 nucleotides (26). Recent data show that the opposite genomic DNA strand at the Wilms' tumour suppressor gene (*WT1*) locus encodes conserved multiple antisense RNAs that may regulate WT1 expression via RNA:mRNA interactions, and which are deregulated by epigenetic defects and are abnormal in carcinogenesis (44).

In the present investigation we provide evidence both from *in silico* and *in vitro* analyses that HAS2 mRNA and HAS2-AS1 RNA interact by heteroduplex formation. The predominantly cytoplasmic localisation of the RNA:mRNA duplex that we observed has also been reported at the *WT1* locus (44). The formation of HAS2-AS1:HAS2 duplexes raises the possibility that HAS2 expression might be affected differently due to the sequence variation in L- and S-HAS2-AS1 transcripts. We intend to pursue this line of investigation further in future studies of the RNA:mRNA interaction, while bearing in mind that additional levels of regulation of gene expression by noncoding RNAs continue to come to light (e.g. 45, 46).

In summary, we have identified expression in PTC of the previously-described natural antisense for the human HAS2 gene, HAS2-AS1. Coordinated temporal profiles of transcriptional induction of HAS2-AS1 and HAS2 were observed in response to stimulation with IL-1β or TGF-β1. In each case, IL-1β induction was blunted following siRNA knockdown of Sp1 and Sp3, while pre-treatment with siRNAs for Smad2 and Smad3 suppressed TGF-β1-stimulated up-regulation of both RNAs. The use of HAS2-AS1-specific siRNAs inhibited the up-regulation of both antisense RNA and HAS2 mRNA by IL-1β. Endpoint RT-PCR revealed the expression of L- and S-HAS2-AS1 splice variants that differ only in their length of sequence complementarity with HAS2, and provided evidence of HAS2-AS1 RNA:HAS2 mRNA duplex formation. We suggest that these data infer a role for HAS2-AS1 in the stabilisation or augmentation of HAS2 expression in PTC. Furthermore, the presence of the above HAS2-AS1 splice variants provides evidence of a potential additional level of regulation of HAS2 expression in these cells by formation of heteroduplexes of different lengths.

REFERENCES

1. Lee, J. Y., and Spicer, A. P. (2000) *Curr. Opin. Cell Biol.* **12**, 581-586
2. Andhare, R. A., Takahashi, N., Knudson, W., and Knudson, C. B. (2009) *Osteoarthritis Cartilage* **17**, 892-902
3. Bharadwaj, A. G., Kovar, J. L., Loughman, E., Elowsky, C., Oakley, G. G., and Simpson, M. A. (2009) *Am. J. Pathol.* **174**, 1027-1036
4. Itano, N., and Kimata, K. (2008) *Semin. Cancer Biol.* **18**, 268-274
5. Lauer, M. E., Mukhopadhyay, D., Fulop, C., de la Motte, C. A., Majors, A. K., and Hascall, V. C. (2009) *J. Biol. Chem.* **284**, 5299-5312
6. Milner, C. M., Higman, V. A., and Day, A. J. (2006) *Biochem. Soc. Trans.* **34**, 446-450
7. Toole, B. P. (2004) *Nat. Rev. Cancer* **4**, 528-539
8. Wight, T. N. (2008) *Front. Biosci.* **13**, 4933-4937
9. Spicer, A. P., Seldin, M. F., Olsen, A. S., Brown, N., Wells, D. E., Doggett, N. A., Itano, N., Kimata, K., Inazawa, J., and McDonald, J. A. (1997) *Genomics* **41**, 493-497
10. Sayo, T., Sugiyama, Y., Takahashi, Y., Ozawa, N., Sakai, S., Ishikawa, O., Tamura, M., and Inoue, S. (2002) *J. Invest. Dermatol.* **118**, 43-48
11. Monslow, J., Williams, J. D., Norton, N., Guy, C. A., Price, I. K., Coleman, S. L., Williams, N. M., Buckland, P. R., Spicer, A. P., Topley, N., Davies, M., and Bowen, T. (2003) *Int. J. Biochem. Cell Biol.* **35**, 1272-1283
12. Gressner, O., Weiskirchen, R., and Gressner, A. (2007) *J. Cell. Mol. Med.* **11**, 1031-1051
13. Nobili, V., Parkes, J., Bottazzo, G., Marcellini, M., Cross, R., Newman, D., Vizzutti, F., Pinzani, M., and Rosenberg, W. M. (2009) *Gastroenterology* **136**, 160-167
14. Li, Y., Rahmanian, M., Widstrom, C., Lepperdinger, G., Frost, G. I., and Heldin, P. (2000) *Am. J. Respir. Cell Mol. Biol.* **23**, 411-418
15. El-Chemaly, S., Malide, D., Zudaire, E., Ikeda, Y., Weinberg, B. A., Pacheco-Rodriguez, G., Rosas, I. O., Aparicio, M., Ren, P., MacDonald, S. D., Wu, H.-P., Nathan, S. D., Cuttitta, F., McCoy, J. P., Gochuico, B. R., and Moss, J. (2009) *Proc. Natl. Acad. Sci. U. S. A.* **106**, 3958-3963
16. Rouschop, K. M. A., Sewnath, M. E., Claessen, N., Roelofs, J. J. T. H., Hoedemaeker, I., van der Neut, R., Aten, J., Pals, S. T., Weening, J. J., and Florquin, S. (2004) *J. Am. Soc. Nephrol.* **15**, 674-686
17. Lewis, A., Steadman, R., Manley, P., Craig, K. J., de la Motte, C., Hascall, V., and Phillips, A. O. (2008) *Histol. Histopathol.* **23**, 731-739
18. Jenkins, R. H., Thomas, G. J., Williams, J. D., and Steadman, R. (2004) *J. Biol. Chem.* **279**, 41453-41460
19. Meran, S., Thomas, D. W., Stephens, P., Enoch, S., Martin, J., Steadman, R., and Phillips, A. O. (2008) *J. Biol. Chem.* **283**, 6530-6545
20. Jones, S., Jones, S., and Phillips, A. (2001) *Kidney Int.* **59**, 1739-1749
21. Meran, S., Thomas, D., Stephens, P., Martin, J., Bowen, T., Phillips, A., and Steadman, R. (2007) *J. Biol. Chem.* **282**, 25687-25697
22. Monslow, J., Williams, J. D., Guy, C. A., Price, I. K., Craig, K. J., Williams, H. J., Williams, N. M., Martin, J., Coleman, S. L., Topley, N., Spicer, A. P., Buckland, P. R., Davies, M., and Bowen, T. (2004) *J. Biol. Chem.* **279**, 20576-20581
23. Monslow, J., Williams, J. D., Fraser, D. J., Michael, D. R., Foka, P., Kift-Morgan, A. P., Luo, D. D., Fielding, C. A., Craig, K. J., Topley, N., Jones, S. A., Ramji, D. P., and Bowen, T. (2006) *J. Biol. Chem.* **281**, 18043-18050
24. Saavalainen, K., Tammi, M. I., Bowen, T., Schmitz, M. L., and Carlberg, C. (2007) *J. Biol. Chem.* **282**, 11530-11539
25. Makkonen, K. M., Pasonen-Seppänen, S., Törrönen, K., Tammi, M. I., and Carlberg, C. (2009) *J. Biol. Chem*. **284**, 18270-18281

26. Chao, H., and Spicer, A. P. (2005) *J. Biol. Chem.* **280**, 27513-27522
27. Hurst, S.M., McLoughlin, R.M., Monslow, J., Owens, S., Morgan, L., Fuller, G.M., Topley, N., and Jones, S.A. (2004). *J. Immunol.* **169**, 5244-5251
28. Simpson, R. M., Meran, S., Thomas, D., Stephens, P., Bowen, T., Steadman, R., and Phillips, A. (2009) *Am. J. Pathol.* **175**, 1915-1928
29. Hoogendoorn, B., Coleman, S. L., Guy, C. A., Smith, K., Bowen, T., Buckland, P. R., and O'Donovan, M. C. (2003) *Hum. Mol. Genet.* **12**, 2249-2254
30. Frith, M. C., Hansen, U., and Weng, Z. (2001) *Bioinformatics* **17**, 878-889
31. Cartharius, K., Frech, K., Grote, K., Klocke, B., Haltmeier, M., Klingenhoff, A., Frisch, M., Bayerlein, M., and Werner, T. (2005) *Bioinformatics* **21**, 2933-2942
32. Hofacker, W. F., Fontana, W., Stadler P. F., Bonhoeffer, L. S., Tacker M., and Schuster, P. (1994) *Monatshefte für Chemie / Chemical Monthly* **125**, 167-188
33. Bernhart, S. H., Tafer H., Mückstein, U., Flamm, C., Stadler, P. F., and Hofacker I. L. (2006) *Algorithms Mol. Biol.* **1**, 3
34. Livak, K. J., and Schmittgen, T. D. (2001) *Methods* **25**, 402-408
35. Carninci, P., Yasuda, J., and Hayashizaki, Y. (2008) *Curr. Opin. Cell Biol.* **20**, 274-280
36. Mattick, J. S. (2009) *PLoS Genet.* **5**, e1000459
37. Mendes Soares, L., and Valcarel, J. (2006) *EMBO J.* **25**, 923-931
38. Gingeras, T. R. (2007) *Genome Res.* **17**, 682-690
39. Prasanth, K. V., and Spector, D. L. (2007) *Genes Dev.* **21**, 11-42
40. Mercer, T. R., Dinger, M. E., and Mattick, J. S. (2009) *Nat. Rev. Genet.* **10**, 155-159
41. Matsui, K., Nishizawa, M., Ozaki, T., Kimura, T., Hashimoto, I., Yamada, M., Kaibori, M., Kamiyama, Y., Ito, S., and Okumura, T. (2008) *Hepatology* **47**, 686-697
42. Luo, D. D., Fielding, C., Phillips, A., and Fraser, D. (2009) *Nephrol. Dial. Transplant.* **24**, 2655-2665
43. Faghihi, M. A., Modarresi, F., Khalil, A. M., Wood, D. E., Sahagan, B. G., Morgan, T. E., Finch, C. E., St. Laurent Iii, G., Kenny, P. J., and Wahlestedt, C. (2008) *Nat. Med.* **14**, 723-730
44. Dallosso, A. R., Hancock, A. L., Malik, S., Salpekar, A., King-Underwood, L., Pritchard-Jones, K., Peters, J., Moorwood, K., Ward, A., Malik, K. T., and Brown, K. W. (2007) *RNA* **13**, 2287-2299
45. Taft, R. J., Glazov, E. A., Cloonan, N., Simons, C., Stephen, S., Faulkner, G. J., Lassmann, T., Forrest, A. R., Grimmond, S. M., Schroder, K., Irvine, K., Arakawa, T., Nakamura, M., Kubosaki, A., Hayashida, K., Kawazu, C., Murata, M., Nishiyori, H., Fukuda, S., Kawai, J., Daub, C. O., Hume, D. A., Suzuki, H., Orlando, V., Carninci, P., Hayashizaki, Y., and Mattick, J. S. (2009) *Nat. Genet.* **41**, 572-578
46. Taft, R. J., Pang, K. C., Mercer, T. R., Dinger, M., and Mattick, J. (2010) *J. Pathol.* **220**, 126-139

***FOOTNOTES**

**At the beginning of this study, M-yK was a pupil of St John's College, Old St Mellons, Cardiff CF3 5YX, UK, and the recipient of a Nuffield Science Bursary coordinated by Techniquest Science Discovery Centre, Cardiff CF10 5BW, UK. AA was the recipient of a research fellowship from the Libyan Government, RDN the recipient of a PhD studentship from the Cardiff University School of Medicine. For helpful discussions and advice we thank Dr Donald J Fraser and Dr Robert Steadman of the Institute of Nephrology, Cardiff University School of Medicine, as well as Dr Keith W Brown, Dr Anthony R Dallosso and Dr Karim Malik of the Cancer and Leukaemia in Childhood-Sargent Research Unit, Department of Cellular and Molecular Medicine, School of Medical Sciences, University of Bristol, Bristol BS8 1TD, UK. For his very generous help and encouragement on entering the field of hyaluronan research, TB expresses particular gratitude to Dr Andrew P Spicer, discoverer of HAS2-AS1.

[1]The abbreviations used are: ATRA, *all-trans* retinoic acid; BACE-1, β-site amyloid precursor protein-cleaving enzyme 1; ECM, extracellular matrix; HA, hyaluronan (hyaluronic acid); HAS, hyaluronan synthase; HAS2-AS1, hyaluronan synthase 2 antisense 1; HK-2, human kidney cell line 2; IL, interleukin; iNOS, inducible nitric oxide synthase; kb, kilobase pairs; L-HAS2-AS1, long HAS2-AS1 isoform; NF-κB, nuclear factor-κB; PTC, renal proximal tubular epithelial cell; qRT-PCR, quantitative (real-time) reverse transcription-PCR; RARE, retinoic acid response element; rRNA, ribosomal RNA; RT, reverse transcription; S-HAS2-AS1, short HAS2-AS1 isoform; siRNA, small interfering RNA; Smad, homologue of *Drosophila* protein mothers against decapentaplegic (MAD); Sp, specificity protein; TGF, transforming growth factor; TFBS, transcription factor binding site.

FIGURE LEGENDS

FIG. 1. **Genomic organisation of HAS2-AS1 and HAS2 at locus 8q24.13, and locations of consensus TFBS motifs and primer binding sites for luciferase reporter, endpoint RT-PCR and qRT-PCR analyses of the human *HAS2-AS1* gene.** *A*, the four exons of HAS2-AS1 on the upper (+) strand of chromosome 8 at locus 8q24.13 are shown as filled boxes, with the transcription start site illustrated as an arrow. HAS2 on the lower (–) strand is depicted similarly, and the overlap of HAS2-AS1 exon 2 and HAS2 exon 1 is evident. The sequences displayed in Fig. 1*B* are highlighted in Fig. 1*A* by four grey boxes on the scale bar. *B*, The complete HAS2-AS1 cDNA sequence NR_002835 (26) is shown from 5' terminus at nucleotide +1 to 3' terminus at +1,656 in *upper case*, with the following exceptions. Exon boundaries are numbered and delineated by vertical lines and arrows, e.g. <2|3> for the boundary between HAS2-AS1 exons 2 and 3. Oligonucleotide primer sequences and primer binding site positions are displayed with orientation and labelled as described below. Primer positions for SYBR Green qRT-PCR analyses are shown in lower case and labelled: SYBR-F, qRT-PCR sense-strand primer; SYBR-R, qRT-PCR antisense-strand primer binding site; SYBR-RT, RT antisense-strand primer binding site; aqSYBR-F, absolute quantification qRT-PCR sense-strand primer; aqSYBR-R, absolute quantification qRT-PCR antisense-strand primer binding site. Endpoint RT-PCR primer positions are underlined and labelled A-G (including AR) with the exception of primer E, which overlaps for some of its length with primer D, and the relevant sequence is *italicised*. The alternatively spliced nucleotides in HAS2-AS1 exon 2 are *emboldened*. Upstream of NR_002835 is genomic sequence from -1 to -800. Selected discrete putative TFBSs identified by *in silico* analysis (30, 31) are shown in *upper case*. The NF-Y/CCAAT site around -100 is shown in *italics*, and the overlapping NF-κB motif is shown wholly in *upper case*. Sense-strand PCR primer sequences for the amplification of luciferase reporter construct inserts spanning approximately 0.1 - 0.7 kb of putative HAS2-AS1 promoter sequence are underlined and labelled accordingly, and the common antisense-strand primer binding site is labelled R.

FIG. 2. **Endpoint RT-PCR detection of HAS2-AS1 transcription, optimisation of SYBR Green qRT-PCR and absolute quantification of HAS2 and HAS2-AS1 RNAs.** *A*, Detection of HAS2-AS1 expression in PTC by endpoint RT-PCR using primers A and AR (see Fig. 1*B* for details of all HAS2-AS1-specific primers not used in duplex detection). *B*, From left to right, pairs of HAS2-AS1 qRT-PCR profiles are shown following amplification using primers SYBR-F and SYBR-R from 2 μg, 1 μg, 500 ng and 250 ng of input RT product, respectively. Each pair comprises amplifications from RT reactions carried out using either 0.1 or 1.0 μM of primer SYBR-RT. Profiles for negative control reactions with no reverse transcriptase, no RNA and no cDNA are contained within a box that is highlighted by an asterisk. *C*, Melting curve of HAS2-AS1 SYBR Green amplification products shown in *B*, the negative control reaction range is illustrated by a bracket highlighted by an asterisk. *D*, Variation in Ct in the presence of different quantities of input RNA (see *B*, above) and the different concentrations of HAS2-AS1-specific RT primer displayed in the key. *E*, Absolute quantification of copy number of HAS2 mRNA, using primers aqHAS2-F and aqHAS2-R (see text for details), and HAS2-AS1 RNA, using primers aqSYBR-F and aqSYBR-R, in unstimulated cells (empty bars) and in response to stimulation with IL-1β (1 ng/ml) for 3 h (filled bars). Data are displayed from one of two replicate experiments, each carried out in quadruplicate, and error bars show standard error of the mean.

FIG. 3. **Cytokine-stimulated up-regulation of HAS2-AS1 and HAS2 expression is coordinated.** *A*, relative expression of HAS2-AS1 RNA and *B*, HAS2 mRNA in response to IL-1β (1 ng/ml) stimulation; and of *C*, HAS2-AS1 RNA and *D*, HAS2 mRNA following addition of TGF-β1 (10 ng/ml). Data are shown from one of two replicate experiments, each carried out in triplicate, and error bars show standard error of the mean. Significance levels of $p<0.05$ are shown with an asterisk.

FIG. 4. **HAS2-AS1 proximal promoter constructs exhibit constitutive luciferase activity**. The ratio of firefly:*Renilla* luciferase activities for each promoter construct is normalised relative to the promoterless pGL-3 basic construct, labelled C. The promoter constructs are labelled in accordance with the approximate length of putative HAS2-AS1 promoter that they amplify, as shown in Fig. 1*B*. Data are displayed from one of three replicate experiments, each carried out in triplicate, and error bars show standard error of the mean. Significance levels of $p<0.05$ are shown with an asterisk.

FIG. 5. **IL-1β–stimulated up-regulation of HAS2-AS1 and HAS2 is mediated by Sp1 and Sp3; TGF-β1–stimulated up-regulation of HAS2-AS1 and HAS2 is mediated by Smad2 and Smad3.** *A*, relative expression of HAS2 mRNA and *B*, HAS2-AS1 RNA in response to IL-1β (1 ng/ml) stimulation for 3 h; and of *C*, HAS2 mRNA and *D*, HAS2-AS1 RNA following addition of TGF-β1 (10 ng/ml) for 48 h. Empty bars represent unstimulated PTC and filled bars cytokine-treated cells. Target gene siRNAs were used at 30 nM and scrambled siRNA, labelled SCR, at 60 nM. Data are displayed from one of two replicate experiments, each carried out in triplicate, and error bars show standard error of the mean. Significance levels of $p<0.05$ are shown with an asterisk.

FIG. 6. **siRNA knockdown of HAS2-AS1 down-regulates HAS2 transcription.** *A*, relative expression of HAS2-AS1 RNA and *B*, HAS2 mRNA in response to the presence of IL-1β (1 ng/ml) for 3 h following transfection with three different siRNAs designed to knockdown HAS2-AS1 RNA. Empty bars represent unstimulated PTC and filled bars cytokine-treated cells. HAS2-AS1 siRNAs were used at 30 nM, scrambled siRNA, labelled SCR, at 30 nM. Data are shown from one of four replicate experiments, each carried out in triplicate, and error bars show standard error of the mean. Significance levels of $p<0.05$ are shown with an asterisk.

FIG. 7. **Organisation of HAS2-AS1 and HAS2 exon 1 at locus 8q24.13, and endpoint RT-PCR amplification of L- and S-HAS2-AS1-specific fragments from total RNA.** *A*, exons of HAS2-AS1 sequence NR_002835 are depicted as open boxes with the exception of HAS2-AS1 exon 2, where the alternatively-spliced section is shown as a filled box. The HAS2-AS1 exon 1 arrow shows the direction of transcription. Exon 1 of HAS2 NM_005328 plus AJ_604570 (22) is shown as a box defined by dashed lines, as is the arrow which shows the direction of HAS2 transcription. The location of HAS2 genomic regions is labelled on the line above. *B*, Endpoint RT-PCR shows that L- and S-HAS2-AS1 are expressed in PTC. L- and S-HAS2-AS1 RNAs are represented as labelled boxes above and below the RT-PCR data. Endpoint RT-PCR products are displayed as bands on agarose gels following staining with ethidium bromide and labelled according to the primers used for their amplification and which are displayed in Fig.1*B*. A double-stranded DNA size marker is also shown.

FIG. 8. **RNA duplex modelling and detection.** *A*, computed minimum free energy secondary structure of the heterodimer of L-HAS2-AS1 RNA (green) and HAS2 mRNA (red) showing the duplex formed by regions of perfect complementarity and *B*, detection of ribonuclease- and deoxyribonuclease-resistant cytoplasmic RNA duplex by RT-PCR with primers designed to amplify transcription outside (*a*; 5'-cttcgagcagcccattgaac-3' and 5'-agcctgtggaagactcagca-3') or within (*b*; 5'-aaacagttgccctttgcatc-3' and 5'-tgatttgtctctgcccatga-3') the predicted region of L-HAS2-AS1:HAS2 heteroduplex formation.

A)

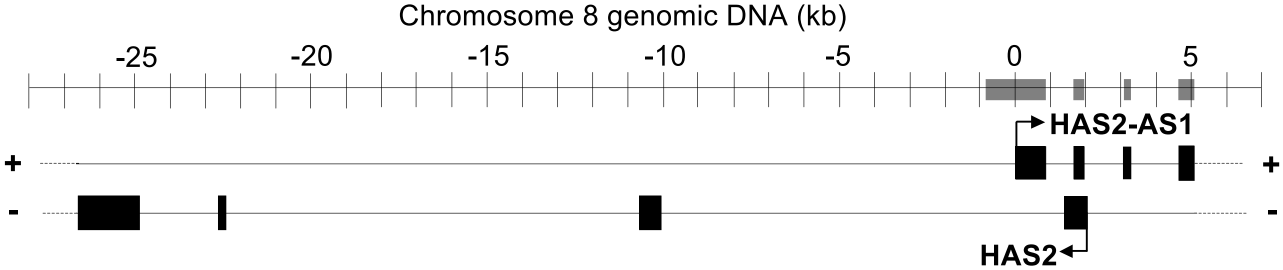

B)

```
                                                                                      0.7>
-800  tactttagttacaatattttgttctagaaatgtccacttaaaaatcagaattatctgtcccagaattggaaacacatacaaaacataatatataaacgca
                                                                                     0.6>
-700  acaggtaacttaaagtgttaaattgtcattgaaaatgtaaaagaatcgccaaactattgggaaaactttggtggagtatgatgggtactcaaaatacag
                                                                                                  0.5>
-600  tacctcagctgtactgtaaccttattaagctctagaaaaatgtggtgaaaactaatttaatgaatgagtcaacttgcacacattggaaggaaataaaaat
-500  ttggaatttaaaagttcttttcaattcaagtcatagaactataaaaaaattgtatctacaaagaggttgatggacttggatctatggaaatacatatttt
           0.4>
-400  aatttaaacctggcatcgtgtatgtaaatatgtgttgaccttttaaaataaccttttaaaaaataataacctggtttaataccgccagaagtactta
                           0.3>
-300  tcatatgccttaaccgcagtgagaaatctgagccaaagccttggaatgtacaatgagcagtgaagttgtctccctcttaacaagcggcctcactccttca
             0.2>                                                                        NF-κB          0.1>
-200  gcaaagcccatctaccaacttccttctctttattctaacactgagctgatggtctatatatactcaggcctccagtTGGGGGAAGCCCTTggtggccaAT
NF-Y/CCAAT | NF-κB             Sp1/Sp3                                   Smad
-100  CGGGGCTTCCCTAtctattgcgtCACACCTCCCCCGtgtgtgacgtcaaaggcaatcccAGCCCAGACacgtgggttggagcagcgtcgcgtttctgggc
      1>          <R
+1    AATTGCTCCTGAAACCCAACAGGCAGCAACGGTCCCAAGGGTGAGGGAGTGGGCAGGGAGAGGCTGATGGGGCTTCTACACGTTCCCTCCCGTAGCTGGG
+101  CTGCTGCAGCTCGTTCGCCCCAGAGGCGCGCGGTGTCCTTGAGTCCAAGTATTCAGCGCGGACGTTTGGGGGACGGAGGGAGAGGCGCTAGGGGAACTGG
                                                                                           SYBR-F>
+201  CACCTAAGACTGTGTAATAGGACACAGGTCTTGCAAGTCCTCCTCCCCAGGCACCGCCCCTGTGCTCCCAGcgcctctttgcagctttaatTATCCTTTC
                              <SYBR-R
+301  AGCGCCGTTCCCCCGCGGCTGCgtttccgtggtcagaggaaaAAGGCTCTTTCGCCTCCCGGTTCTCACCCTCATACAGACCCTCCTTTCAGACCCGCCC
                                                                                          <SYBR-RT
+401  TCCTGTTCACAGGGACCCATTTCGGAGCCCTGGCTCACGCTGGGCGGGAACTGCCGTGACGAATTCCCCCCaaggtgttgattatccatCCCAACCCAGC
+501  CTCTGGCTTCCCTCCCACCTCCACCCCAGCTCCCACAGGCCCCTCGCCCCGTTCATCGGCTGGGCGCTCGAGACGGCGCCCCCAGATCTCCCACCGGGCA
+601  GTGTCCCCAGCTGCAGCTGAGGAGAGAAGCGCCGGCGTGCGCGGTGCCACGTCGGAATTGGCTCTGGGGACGCCGCAGCTGCCGAAGCGCAGCGCGCGGT
                                                                                    A>
+701  CCCCACGCACGCCCTGCCTCCGGGCGGCCGGCGGGCTGGCCCGGCGAGGAGAGGAGGGATGCGCGCCCTCCTCCCGCTCCTATCTGCGGGTGCCACCGCC
                        <1|2>
+801  TGCGTCAGGGACCCCTGGCCCGATCTTTCTGCCCCCGATAACAGAAAATCTCTTTTTCGTCTTAAAAAAAAAAAAAAAAAAAAAAAAAGCCTGTGGAAGA
                                                                                                  <D|E>
+901  CTCAGCAGAACCCAGGAAGCGCAGAATTGGGAGAAAAGTCTTTGGCTGGGGCTGTTTCAAGTCTCTGGTTCAATGGGCTGCTCGAAGCCAGGACTGGGTA
                     B>                                     <C                        <2|3>    <D|E>
+1001 ATTCTTTCCAGACGTCTTGACTTCTCCTTCCCCGCCGTTGTTGCCCTTCTGCCTCCTCCAACTTAAGGGGGTCTTAACAAGATCTTCTGAGGGGTGGACT
                         <AR                                                                  aqHAS2-AS1-F>
+1101 TCTTTGGAACTCGACAGGACCTTGAAGACTGGGTTCTTAGTCCTTATCACATATATGGGCTATAATGAATAAGTCTAAACAGAAAAGtcgaataaactgg
                                <3|4>                                            <aqHAS2-AS1-R
+1201 aaatgatgcTTTCATCACGTCGCACAAGGAGCTGTTTGGATCAGAAGATGACATCCTTTCACCCatccctttcaggttttgacatcCTAAAATGTACCTT
              <
+1301 ATGGAACCCATACCTGTTATGTTTTCACCTGTACAAGGCAACAGAGAAAACATGGTAGTTTTTACTTGAGTAGATGTGACTTAGCAATATGTTGTTGCTG
+1401 ACCTCCATCCCACAGCACAAAACATATGTTTATATGTCTGACAGACAAAGTATCCAGAACAAGGATTTAGTACCTTCATAATCCTCTGTATATGTGGTTC
+1501 TAGAACTTTTGGTAAAGAAACTCTTTATACTCTTATTAATTATTGAGAACCTCAAAAAAAGTTTATATGTTATATGTATCAATATTTACCACATTAGACA
                                                            <4
+1601 TTAAAGCTGACTTAAAAAGTTAAAATACTTAAGTCATTTGAAGTAATAATAAATGC
```

Figure 1

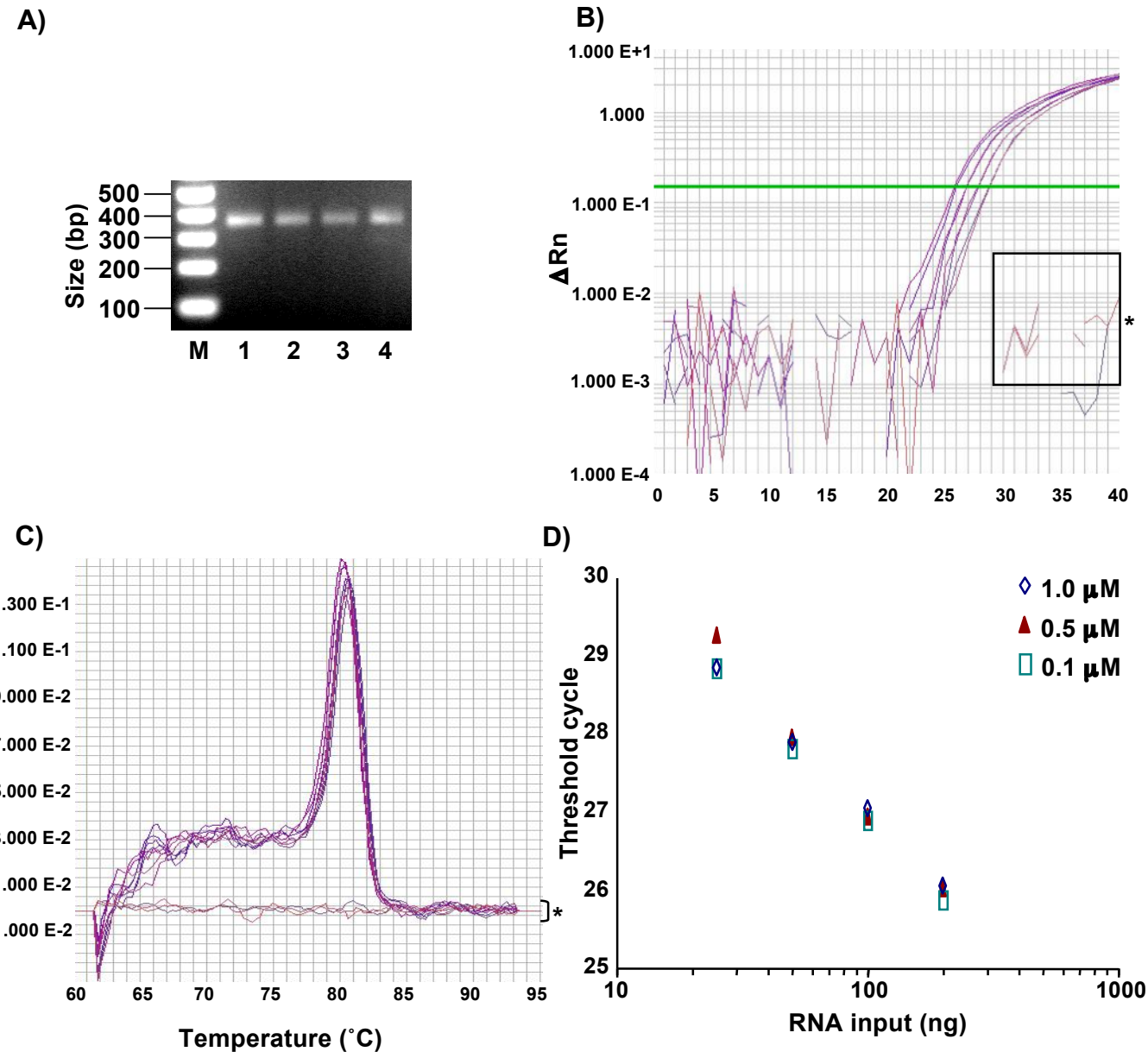

Figure 2

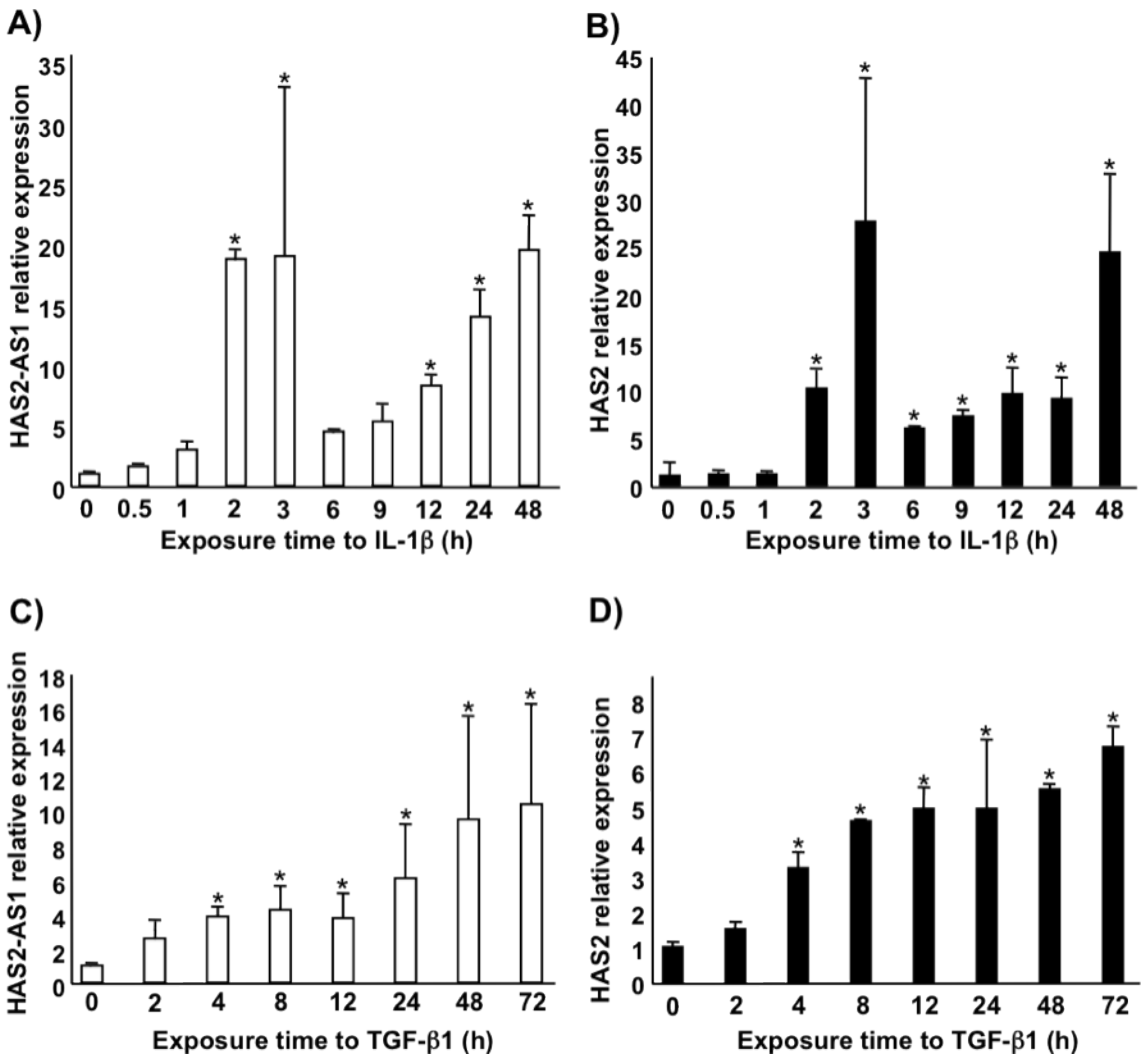

Figure 3

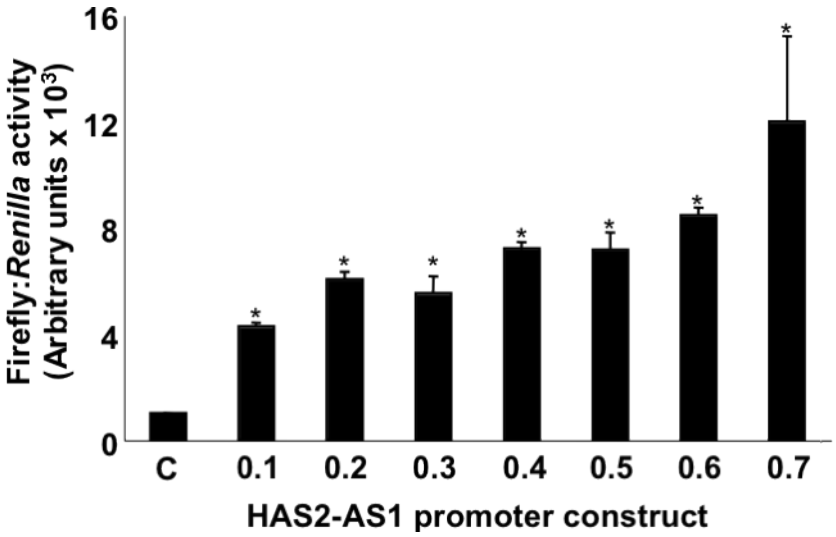

Figure 4

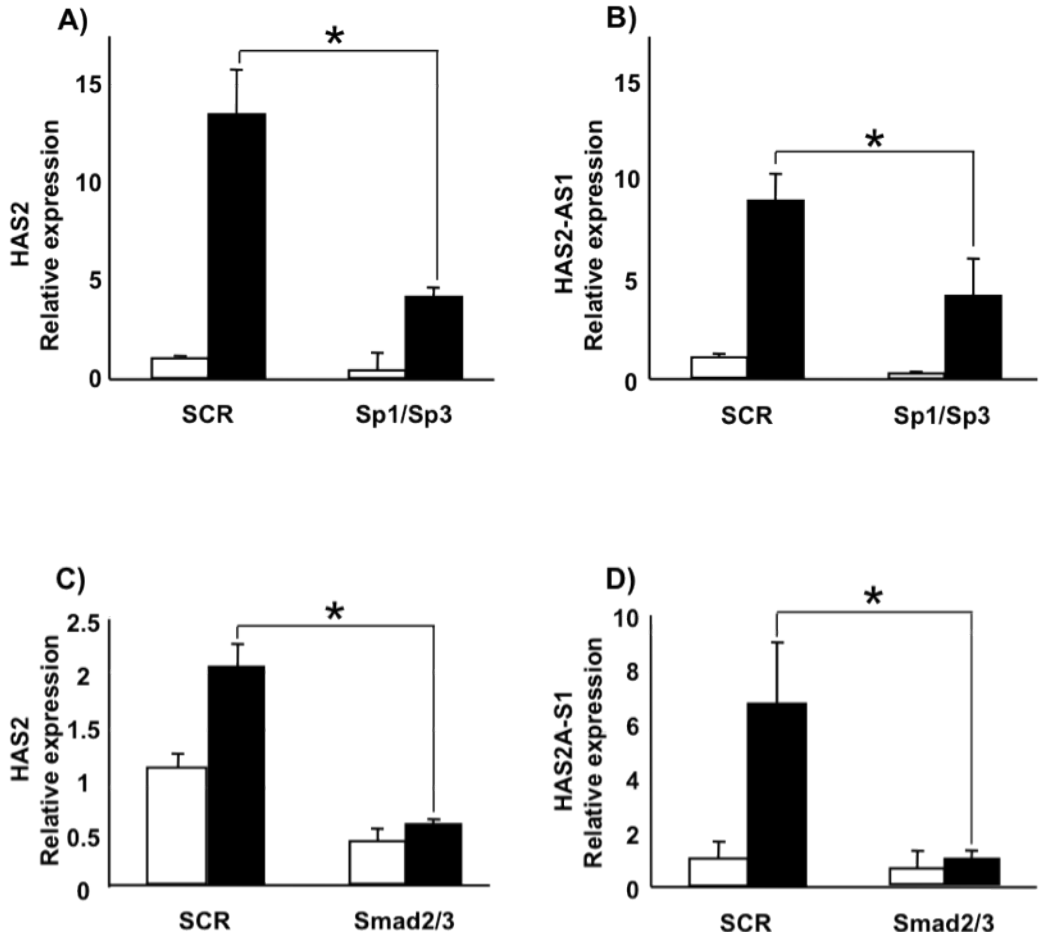

Figure 5

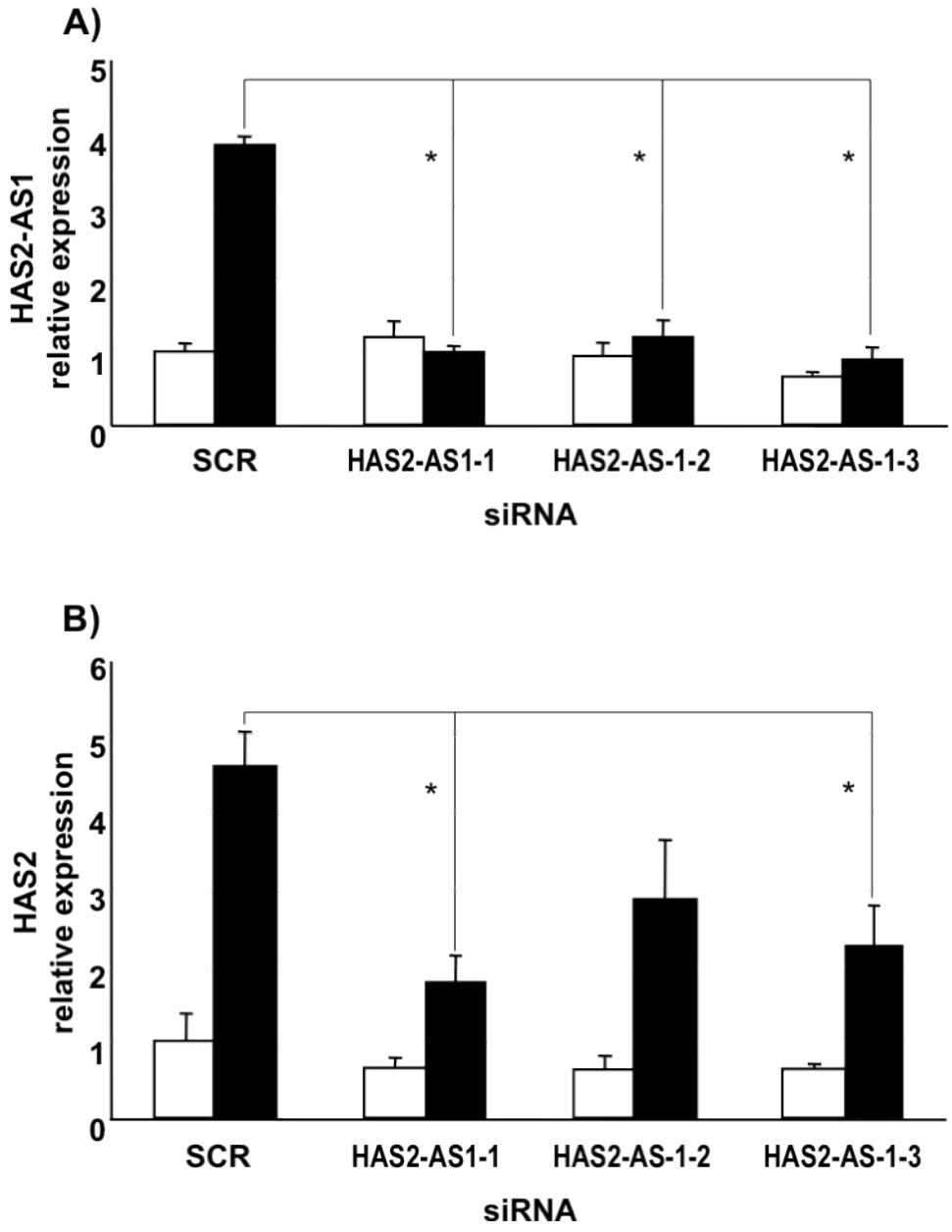

Figure 6

A)

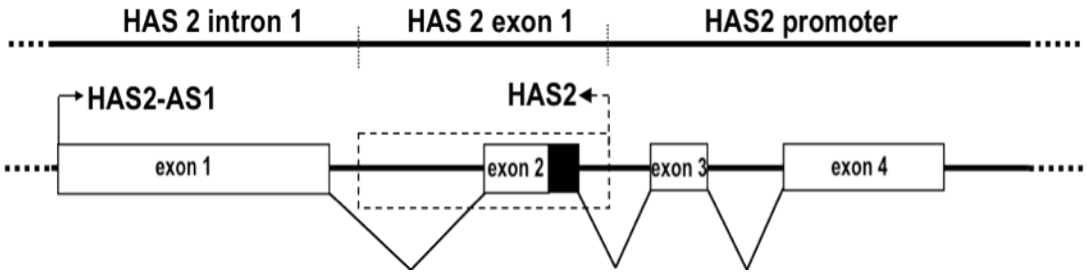

B)

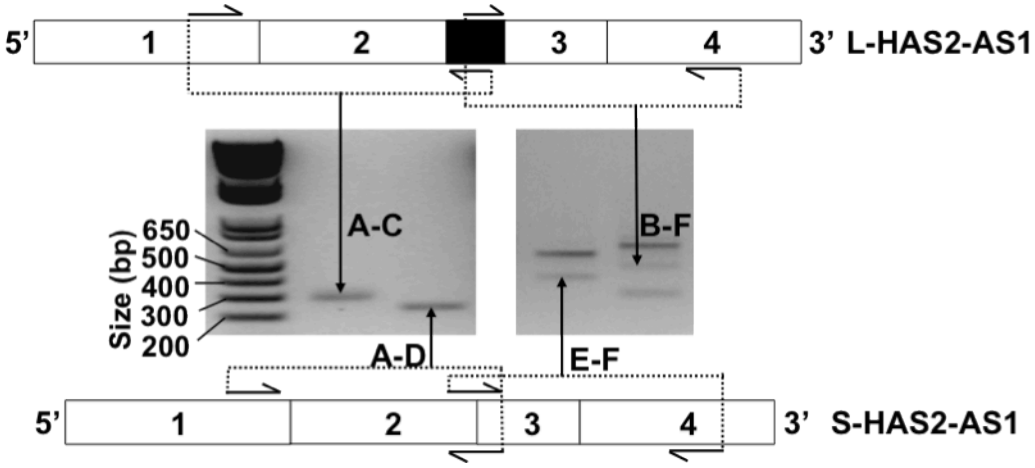

Figure 7

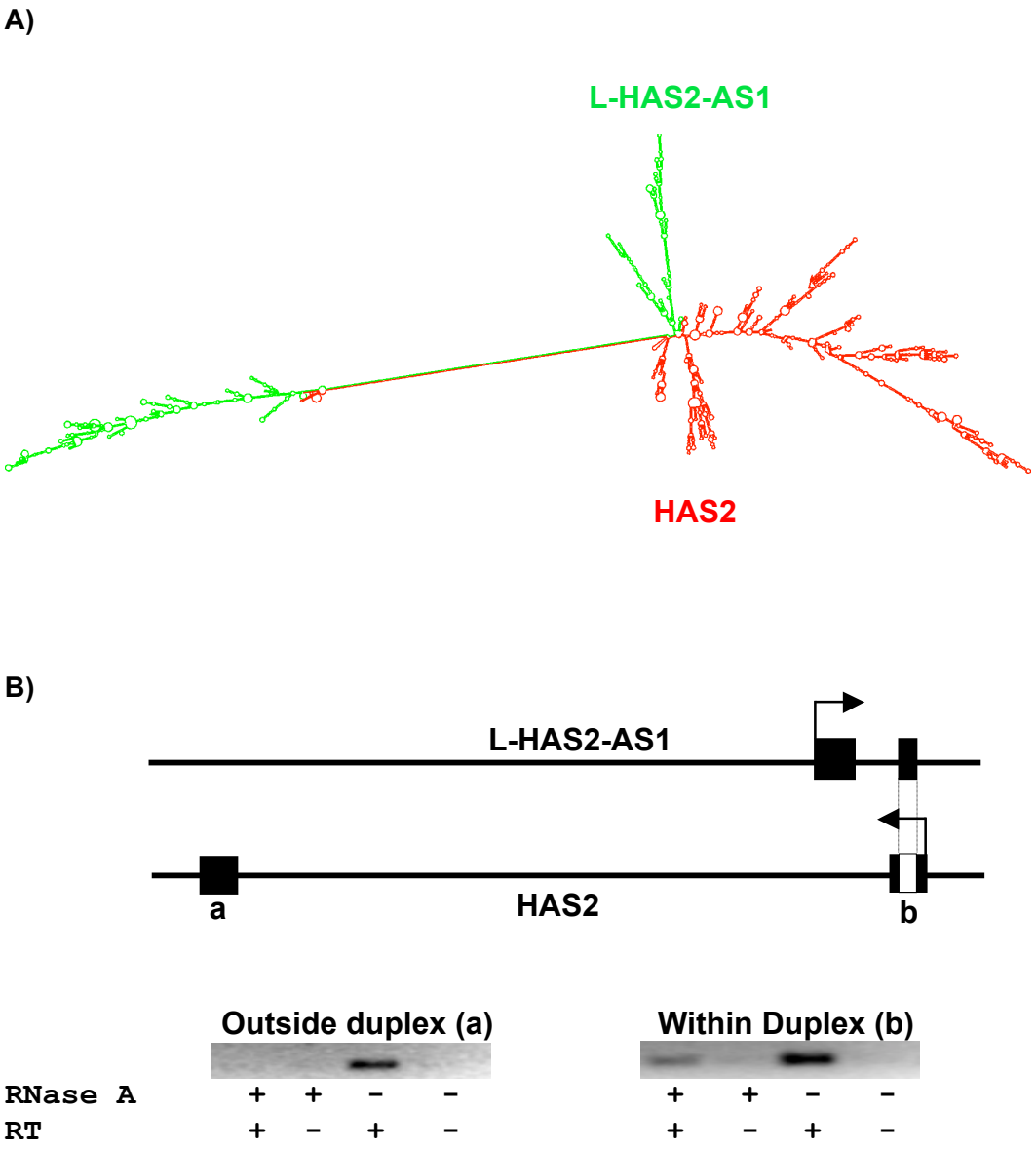

Figure 8